I&EC research
Industrial & Engineering Chemistry Research

pubs.acs.org/IECR

Article

Process Simulation Modeling of the Linear Low-Density Polyethylene Catalytic Pyrolysis in a Fluidized Bed Reactor

Sanaa Hafeez, Maarten Van Haute, Achilleas Constantinou,* and Sultan M. Al-Salem*

Cite This: *Ind. Eng. Chem. Res.* 2023, 62, 6386−6393

Read Online

ACCESS | Metrics & More | Article Recommendations

ABSTRACT: In this work, a comprehensive process simulation was developed to study and predict the pyrolysis of linear low-density polyethylene (LLDPE) in a fluidized bed reactor (FBR). The comprehensive simulation operated at 600 and 700 °C to investigate the pyrolytic oil and wax yields. These products were chosen as they mimic fuel range products available as a renewable fuel and energy source. The results showed that the oil yield decreased from 600 to 700 °C. This is because of an increase in the polyolefin polymer matrix's vibration leading to an increase in temperature and absorbed thermal energy. In addition, there is a higher gas yield produced and negligible wax formation at 700 °C, which is beneficial in controlling accrued plastic waste (PW), of which polyethylene (PE) represents a vast proportion of via thermo-chemical conversion (TCC) technologies. The detailed process simulation was compared with experimental data under the same technology and operating conditions, and it was found that less than 10% discrepancy was observed between the two sets of data, suggesting a good validation between the two studies. Further studies showed that the diesel fuel lumped hydrocarbon (HC) range (C_{10}−C_{19}) was between 40 and 63% in the pyrolysis oil yield obtained. Moreover, the temperature profiles and fluidized bed distributor parameters were compared and investigated. The current simulation has proven that it can successfully predict the pyrolysis of LLDPE in an FBR.

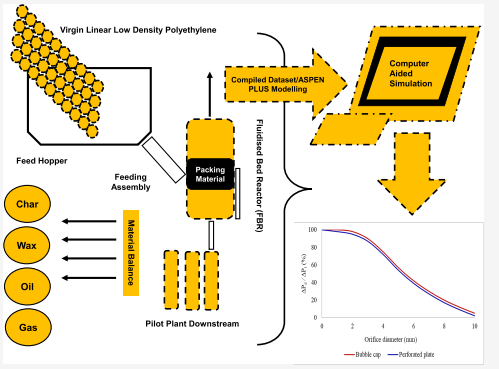

INTRODUCTION

The management of plastic waste (PW) is an imperative problem, particularly in developing countries. The constant increase in plastic production over the last several decades has led to detrimental environmental consequences due to their slow degradation in open environments, release of pollutants, and accumulation.[1] The global production of plastics reached 368 million tons, of which China has contributed 31% back in 2019. Europe's plastic production decreased from 61.8 million tons in 2018 to 57.9 million tons in 2019, and 29.1 million tons of PW was collected for treatment in 2018.[2] PW is also noted to constitute a large proportion of waste in landfill sites estimated on average at 24.9%.[2] Once discarded, PW eventually decomposes and fragments with time into microplastics, which can be absorbed and accumulated by humans and animals through the food chain.[3] The mechanical recycling of solid waste is a viable option; however, the process requires an intense sorting process and leads to water contamination issues.[4] Chemical recycling, such as gasification, pyrolysis, and depolymerization, proposes a more desirable result because of its capability to treat several types of plastics and has a higher tolerance for contamination.[5,6] Gasification is a thermochemical process that transforms carbonaceous matter into a gaseous secondary energy carrier, referred to as product gas, which can be used for heat and power generation but also for syntheses.[7,8] 21 years of study in the circular economy of plastics based on a review of 21 years of previous research has shown that pyrolysis is one of the highly researched chemical recycling methodologies, following PET depolymerization.[7,9]

The pyrolysis of PW has proven to be a popular method of thermo-chemical conversion (TCC) recycling in recent years because it can achieve environmentally friendly conversion of PW into highly valuable fuels and chemicals.[10] The pyrolysis process consists of treating the PW in the absence of oxygen (or a reactive atmosphere) to produce a range of products, such as crude oil-equivalent products, liquid fuels, gas, and solid/char residues.[11,12] The actual composition of the product type is dependent on several factors, notably the type of feedstock and the reaction's operating conditions. The pyrolysis temperature facilitates the degree to which the polymeric chain is broken. Therefore, higher temperatures aid the generation of smaller chained hydrocarbons (HCs) and

Received: December 6, 2022
Revised: March 6, 2023
Accepted: April 3, 2023
Published: April 17, 2023

https://doi.org/10.1021/acs.iecr.2c04379
Ind. Eng. Chem. Res. 2023, 62, 6386−6393

vice versa. Nonetheless, the feedstock establishes the degradation pathways and the resulting chemical composition of the generated products.[13,14] Furthermore, operational factors such as residence time, heating rate, catalyst, and reactor configuration can have a significant effect on optimizing the performance of the pyrolysis process. Catalysts can be implemented to reduce the reaction temperature and energy usage, or microwave assisted reactors can be further utilized to improve the rate of heat transfer.[15]

The type of reactor used in the pyrolysis process has a large influence on important parameters such as mass and heat transfer rates, residence time, mixing ability of reactants and catalysts, and economic efficiency. The fluidized bed reactor (FBR) is designed to address the shortcomings of the fixed bed reactor because it is fitted with a continuous feeding mechanism that aids in producing oil more efficiently. This form of reactor has numerous applications, especially in the oil and chemical industry sectors.[16,17] Furthermore, they offer a more enhanced mass and heat transfer and decrease temperature gradients throughout the reactor.[18−20] The mass and heat transfer are improved due to the better mixing of the catalyst with the fluid, which provides a greater surface area for the reaction to occur. Qianshi et al.[21] developed a theoretical model of biomass char gasification focusing on the catalytic effect of inorganic elements on the char gasification process. The result from a previous work shows that the catalytic ability of potassium in a fixed bed reactor is stronger than that of calcium, while the catalytic ability of calcium in an FBR is stronger than that of potassium. For the FBR, a higher proportion of calcium is transformed into an ion-exchanged state than potassium, as opposed to the experimental results in the fixed bed reactor. It was concluded that the model can effectively predict the reactivity of char gasification in accuracy and trend.

Salaudeen et al.[22] studied the pyrolysis of high-density polyethylene (HDPE) in a novel FBR. The reaction system can be adapted to a range of TCC methods including pyrolysis, gasification, and combustion. Catalytic conversion and co-conversion of different feed materials can also be performed in the reactors. The results showed that wax was the dominant product at 500 °C, and the addition of the Magnofil (olivine) catalyst increased the wax yield from 45.6 to 66 wt % and promoted the formation of olefins. Furthermore, pyro-wax has a high energy content (44.82 ± 0.24 MJ kg^{-1}) and can be a potential source of fuel, and the heating value was like that found in conventional fuels.

A further study conducted by Al-Salem et al.[23] investigated the pyrolysis of virgin linear low-density polyethylene (LLDPE) using an FBR in an average temperature range between 600 and 700 °C with a catalyst-to-oil ratio of 2.6 and 2.4. respectively. The results show that at 700 °C, there was no amount of wax produced; however, larger quantities of pyrolytic oil and gas yield were produced, which provides a promising solution to the management of accumulated PSW. Furthermore, it was found that the calorific value observed was approximately 45.5 MJ kg^{-1} at 600 °C, which is in the desirable range for gasoline and diesel fuel market value. It was concluded that the experimental results from the pilot-plant work depicted in this study are encouraging for the integration of sustainable fuel alongside current petroleum production companies soon.

Despite the popularity of pyrolysis of plastics for fuel production, most researchers have focused on determining product compositions using experimental methodologies. Only a handful of past studies have used computational modeling to validate and predict the pyrolysis reactions.[24−26] Performing numerical studies using a computational software is beneficial as it provides an understanding of parameter optimization for the pyrolysis of plastics, which is currently not well established.

In this work, the pyrolysis of LLDPE is investigated using process simulation modeling using Aspen Plus in a novel recently patented FBR system developed by Al-Salem et al.[23] The novelty lies in the fact that the FBR has been reported to promote oil yield at low pyrolysis temperatures, reducing the energy requirement of the process. Hence, in addition to thermal decomposition, the catalyst would promote the catalytic cracking of HCs in PW. The theoretical model will be based upon and validated against previous experimental work studying the pyrolysis of LLDPE in the FBR.[23] The comprehensive process simulation will determine the oil and wax products at 600 and 700 °C and investigate the properties of this range of fuel produces using a catalytic FBR system, which can provide a promising pathway for PSW management via pyrolysis. The current work is highly novel as the computational modeling on the pyrolysis of LLDPE in a FBR system is not widely reported in literature. For the first time, the study is conducted using an innovative FBR experimental setup developed by the research group of ref 23 for this specific feedstock rich in PW. The computational model has proven a good validation with the experimental results and therefore can be adapted to investigate the pyrolysis of different feedstocks.

Mathematical Modeling Methodology and Structure.

The FBR utilized sand (90 vol %) as the fluidized bed material alongside the bed additive catalyst (Magnofil, 10 vol %), with weights of 1717 and 168 g, respectively.[23] Typically, metal oxide, particularly alkali and alkali earth metal (AAEM) oxides, have been extensively investigated in the past two decades and are becoming increasingly popular due to their high catalytic performance and low costs.[27−29] However, the lack of inexpensive and effective catalysts limits the development of catalytic pyrolysis for PWs. Olivine (e.g., Magnofil) has been extensively used as a tar cracking agent in PW conversion.[30] It has been reported to promote oil yield at low pyrolysis temperatures, reducing the energy requirement of the process.[31] Hence, in addition to thermal decomposition, Magnofil would promote the catalytic cracking of HCs in PW. For these reasons, and considering that Magnofil is a low-in-price natural mineral, the pyrolysis experiments were conducted with this catalyst. The FBR study was performed with operating temperatures of 600 and 700 °C. The mass of the sample fed continuously in the reactor was 5 kg, with a nitrogen (N_2) flow rate of 10 L min^{-1}.[23] Further experimental details are available in Al-Salem et al.'s study[23] including the pressure drop and other handling protocols of the pilot plant.

For the mathematical modeling of the FBR in Aspen Plus, a solid template is selected to solve the boundary conditions. The method filter selected is all, and the base method is solids. The component feedstock selected is LLDPE. The fluid packages selected to solve the complex mathematical problems were Peng Robinson with RK-Aspen (*Redlich−Kwong*), as they can accurately predict the vapor−liquid equilibrium data of HCs at high temperatures and pressures. Following the completion of component and methods selection, a physical and thermodynamics methods check is run, and the physical property analysis calculations are completed normally. The

https://doi.org/10.1021/acs.iecr.2c04379
Ind. Eng. Chem. Res. 2023, 62, 6386−6393

fluidized bed unit is selected to perform the modeling validation studies, consisting of two solid and two fluid streams. The reactor bed region has an internal diameter of 102.76 mm and entire length of 1500 mm. Table 1 displays the parameters used for the pyrolysis process.

Table 1. Parameters Used for the Process Simulation Modeling

symbol	value	units	description
T	600, 700	°C	operating temperature of FBR
D_i	0.103	m	internal diameter of reactor bed[22]
L	1.5		reactor length[23]
ρ_b	1590	kg·m^{-3}	bulk density of fluidizing bed material
ρ_c	1400		bulk density of olivine catalyst
m_b	1.885	kg	mass of fluidizing bed material
F_{N2}	10	L·min^{-1}	flow rate of N_2[23]
m_f	5	kg	total mass of sample for each run

Pyrolysis decomposition kinetics is normally calculated using iso-conversional methods. One of the main principles of iso-conversional methods is that the heating rate and temperature changes do not affect the reaction mechanism.[32] Compared with model-free methods, model-fitting methods obtain more kinetic parameters.[33] The Coats−Redfern integral method[34,35] is often adopted to calculate the kinetic parameters of LLDPE pyrolysis. In this case, the first-order reaction mechanism is chosen as the basis because it is the primary mechanism.[36] Most kinetic models use the Arrhenius equation and the conversion rate equations. In this case, the Conesa and Font[37] correlation is utilized to perform the kinetic modeling. This is because the pyrolysis in a fluidized-bed reactor of two types of polyethylene is studied using the severity function and considering the primary and secondary yields, setups which are similar to those of the current study.

Fundamentally, and assuming a continuous pyrolysis operation of the feedstock, the mathematical treatment of process parameters is an essential step to understanding the nature of the work conducted in a pyrolysis system. Following the Conesa and Font[37] relationship established for the kinetic severity function (KSF) and in establishing the polymeric degradation mathematical expression, one can assume the following to establish the evolution of primary volatile components from the reactor setup:

$$\frac{dV_{vp}}{dt} = -V_{P,\infty}\frac{dPE}{dt} \tag{1}$$

where V_{vp} is the primary components total volume (m^3) evolved (primary gases + primary waxes and tars), $V_{P,\infty}$ is the highest value, and PE indicates the mass fraction of the polyethylene component. A secondary reaction model is assumed to crack the tars and waxes following a first-order kinetic reaction. The cracking of tars and waxes produced during secondary reaction is obtained by utilizing the following expression:

$$\Delta V_{V2} = \Delta V_{p,0}(1 + \alpha X_S) \tag{2}$$

where ΔV_{V2} is the total volume of gases (primary + secondary) that are within a contained volume ΔV_R, $\Delta V_{P,0}$ is the volatiles volume produced (tars + gases + waxes) when time (t) = 0, X_S is the extent of reaction, and α is an expansion factor that can be determined for every time period. Therefore, it can be stated that the heat transfer between the volatiles and reactor walls is characterized by

$$\frac{dT_p}{dt} = \frac{U_1 S}{c_p}(T_b - T_p) \tag{3}$$

$$\frac{dT_i}{dt} = H_s(T_R - T_i) \tag{4}$$

where T_b is the fluidized bed or reactor bed temperature (K), T_P represents the actual temperature of the sample at time t, and S is the feedstock or the Pes external surface (m^2). The heat transfer coefficient and specific heat capacity can be represented by U_1 (Js^{-1} m^2 K) and c_p (J kg^{-1} K^{-1}), respectively. T_i is the real temperature of the volume studied, T_R is the reactor temperature corresponding to the temperature profile determined at the volume position, and H_s is a fitting parameter (s^{-1}). The minimum fluidization velocity is computed using the Ergun equation thus:

$$u_{mf} = 7.14(1 - \varepsilon_{mf})\gamma_g S_V\left[\sqrt{1 + 0.067\frac{\varepsilon^g mf}{(1-\varepsilon_{mf})^2}\frac{(\rho_s - \rho_g)}{\rho_g \gamma_g^2}\frac{1}{S_v^g}} - 1\right] \tag{5}$$

where ρ_g and γ_g are the gas density (kg m^{-3}) and dynamic viscosity (Pa s), respectively; ρ_s is the particle density; ε_{mf} is the bed porosity at minimum fluidization; and S_v is the volume-specific surface area. The superficial gas velocity u_g (m s^{-1}) is given by

$$u_g = \frac{m_g}{\rho_g(T_i p)A} \tag{6}$$

The pressure drop (Pa) across the bed Δp_{fb} and the distributor Δp_{dis} is expressed by the following equations:

$$\Delta p_{fb} = H(1 - \varepsilon)\rho_s g + H\varepsilon\rho_g g \tag{7}$$

$$\Delta p_{dis} = \left(\frac{u_{or}}{c_{dis}}\right)^2 \frac{\Delta P_g}{2} \tag{8}$$

The Tasirin and Geldart[38] model is applied for elutriation as per the following:

$$k_{i,\infty} = A \cdot e^{(B.^u t/u)} \cdot \rho_g u \tag{9}$$

where $k_{i,\infty}$ is the elutriation coefficient and $u_{t,I}$ is the particle terminal velocity.

RESULTS AND DISCUSSION

Model Validation. The mass balance of the lumped averaged products (e.g., pyro-oil, char, wax, and gas) of the pyrolysis reactions is shown in Table 2 after the extensive experimental campaign conducted prior and shown in Al-Salem et al.[23] In order to assess the validity of the process simulation, the process simulation data were compared to the experimental results obtained,[23] which is compiled as such and shown in Figure 1. It was observed there is a less than 10% discrepancy between the experimental data obtained for the product mass balances and the process simulation modeling data. Therefore, the process simulation model has demonstrated good validity with the experimental work. The mass

https://doi.org/10.1021/acs.iecr.2c04379
Ind. Eng. Chem. Res. 2023, 62, 6386−6393

Table 2. Experimental Data of the Material Balance Established in the FBR Pilot Plant[a]

material balance: FBR pilot plant				
feedstock: (5) kg per run				
avg. reactor temp. (°C)	oil (g)	char (g)	wax (g)	gas (g)
500	6.6	3.8	4301	688.60
600	438.90	4.00	1151.55	3405.55
700	405.95	19.95	0.00	4574.10
percentile (%)				
avg. reactor temp.	oil	char	wax	gas
500	0.132	0.076	86.020	13.772
600	8.778	0.080	23.031	68.111
700	8.119	0.399	0.000	91.482

[a]Data source: Al-Salem et al.[23]

balance and individual product yields were calculated using the following equations:[23]

$$\text{pyrolysis total gas yield\%} = 100 - [\text{total oil\%} + \text{total wax\%} + \text{total char\%}] \quad (10)$$

$$\text{pyrolysis p yield\%} = m_p/m_f \times 100 \quad (11)$$

where m_p and m_f are the weighed pyrolysis product fraction and the total feedstock mass, respectively. The results showed that as the temperature increased from 500 to 700 °C, the total gas yield increased. On the other hand, at temperatures between 600 and 700 °C, the oil yield appeared to decrease slightly. Furthermore, no waxes were produced at higher temperatures of 700 °C; this is due to the thermal degradation of the feedstock, as well as the design of the FBR. Higher temperatures, typically above 550 °C, will result in the accelerated reach of polyolefin polymers to a molten state prior to degradation. This will also increase the evolution of their degressive products (e.g., non-condensable gaseous components) due to primary reaction cracking, which decreases and eventually eliminates wax formation. The maintained temperature of the FBR allows the polymer less time to reach a molten state, which results in delivering waxes up to 600 °C. In the case at hand herein, no wax formation occurred at 700 °C but a high yield of gaseous products and oils was observed, which are more lucrative in managing accumulated PSW via TCC technologies as both gas and oils can be utilized as standalone products or recycled within the FBR system.

Park et al.[39] studied the pyrolysis of waste PE in FBR and found that higher temperatures favor the production of polyolefin (PO) polymers to a liquid phase before degradation. As a result, the generation of descending products is encouraged (i.e., non-condensable gases) because of the primary cracking reactions that take place at the initial stage of degradation. Therefore, wax formation is negligible under these conditions. The design of the FBR upon which the process simulation modeling work is based further prevents wax formation at higher temperatures.[40] This is due to the faster uniform heating of the reactor bed, which allows the polymer to reach a molten state faster, hence preventing wax production at elevated temperatures. This also favors industrial design considerations to avoid pyro-wax formation in actual real-world conditions.

The fuel range HCs with respect to the reactor bed temperature are displayed in Table 3. The results show that the diesel range HCs had the greatest yield (C_{10}–C_{19}); this is in accordance with the experimental data discussed prior.[23] Table 4 shows the comparative yields obtained using the process simulation modeling and experimental work.[23] The generation of polyaromatic hydrocarbons (PAHs) increased with temperature up to 700 °C, which can be attributed to aromatization and rearrangement reactions of the monocyclic and aliphatic compounds anticipated at higher temperatures.[41] The wax sample mostly consists of wax range chemicals, and approximately 30% of these were in the diesel range. As a result, the oil samples should be further processed for prospective integration strategies for petroleum as a route for circular economy. In doing so, PSW can be implemented as a sustainable feedstock for integration plans in the future, which can generate fuel decrease dependence on conventional fossil fuels.

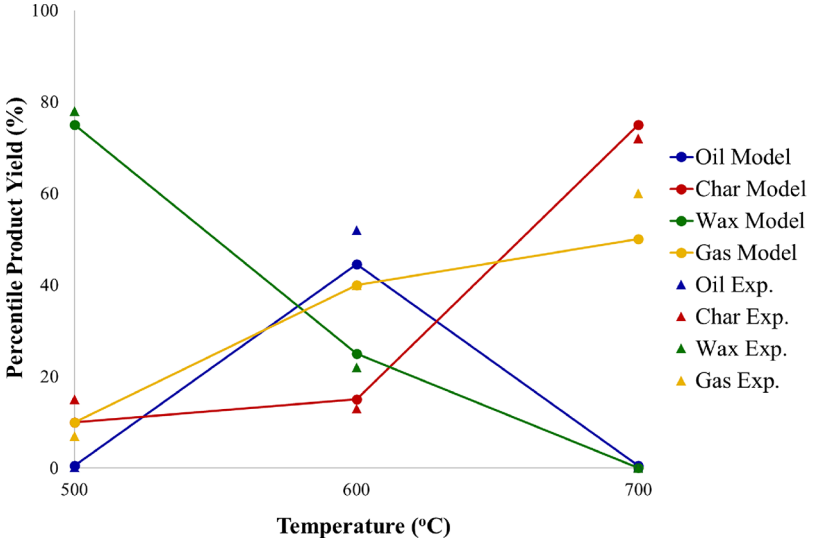

Figure 1. Comparison between the experimental and process simulation modeling displaying the pyrolysis product mass balances compared with the average reactor bed temperature (°C) using process simulation modeling.

https://doi.org/10.1021/acs.iecr.2c04379
Ind. Eng. Chem. Res. 2023, 62, 6386−6393

Table 3. Fuel Potential (Hydrocarbon Range) Estimated for the Pyrolysis Wax and Oil Samples

pyro-oil analysis (600 °C)	run no. 1	run no. 2	run no. 3	run no. 4	avg.	std.	se.
C_6–C_9	16.24	29.64	28.59	18.77	23.31	5.89	2.94
C_{10}–C_{19}	37.56	35.83	34.02	43.11	37.63	3.40	1.70
C_{19+}	46.20	34.54	37.40	38.11	39.06	4.33	2.17
pyro-oil analysis (700 °C)	run no. 1	run no. 2	run no. 3	run no. 4	avg.	std.	se.
C_6–C_9	25.56	25.89	21.44	20.66	23.39	2.36	1.18
C_{10}–C_{19}	58.35	59.24	60.36	65.32	60.82	2.70	1.35
C_{19+}	16.10	14.87	18.20	14.01	15.80	1.57	0.79
pyro-wax analysis (600 °C)	run no. 1	run no. 2	run no. 3	run no. 4	avg.	std.	se.
C_6–C_9	11.23	11.68	24.78	20.67	17.09	5.82	2.91
C_{10}–C_{19}	29.78	26.13	29.71	33.84	29.87	2.73	1.36
C_{19+}	58.99	47.88	45.51	45.49	49.47	5.58	2.79

Table 4. Comparative Depiction of the Mathematical Modeling Results against the Experimental Runs

	modeling results		
	pyro-oil (600 °C)	pyro-oil (700 °C)	pyro-wax (600 °C)
C_6–C_9	21.51	23.02	19.51
C_{10}–C_{19}	39.58	62.55	32.1
C_{19+}	39.48	14.54	48.21
	experimental results		
	pyro-oil (600 °C)	pyro-oil (700 °C)	pyro-wax (600 °C)
C_6–C_9	23.31	23.39	17.09
C_{10}–C_{19}	37.63	60.82	29.87
C_{19+}	39.06	15.80	49.47

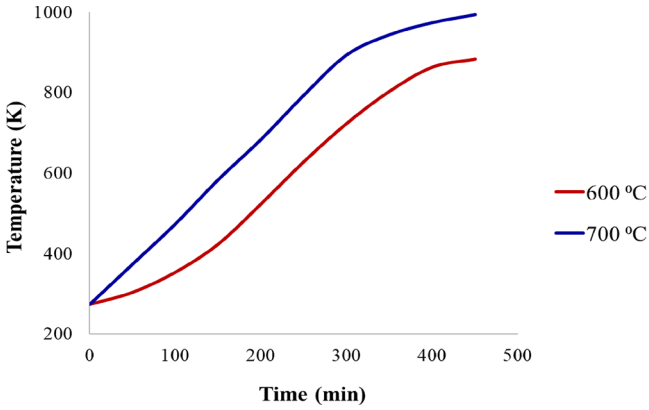

Figure 2. Reactor temperature profile with a total reaction time of 500 min.

The computational model developed has simulated the pyrolysis of LLDPE, which is one major part of the PW observed in global PW streams. Nevertheless, there are several other plastic types, mostly observed in MSW, such as poly(vinyl chloride) (PVC), polypropylene (PP), and poly(ethylene terephthalate) (PET).[42,43] The detailed model can be adapted to predict and test the pyrolysis or co-pyrolysis of several other types of plastic feedstocks to recognize the effects of varying feedstocks on product compositions and yield and the impacts of the type of catalyst used. The pyro-oil yield can be enhanced further by process optimization and by influencing the temperatures of the chiller and cyclone temperature as future work. As a result, this will create the desirable potential to study further the product yields observed when a lower range of operating temperatures is utilized, such as 450 and 500 °C. Subsequently, this can be compared to those yields observed at greater temperatures, e.g., 800 °C.

Effect of Temperature and Distributor Parameters. Figure 2 displays the reactor temperature with time for two distinct temperatures of 600 and 700 °C. The results show that the temperature increased with time to approximately 400 min for each experiment and subsequently stabilized once the desired temperature had been reached. This is in accordance with the experimental data.[23] With temperature increasing, activation energy decreases patently, and it can help to increase the number of chains breaking and decrease the residence time. The high temperature is supplied to the reactor to aid the highly endothermic primary cracking reactions; the high temperatures were then maintained to progress with the cracking reactions. At higher temperatures, the PO molecules were broken down into smaller ones to obtain the fuel range products.

The distributor design parameters can affect and determine how the FBR operates. During the process simulation modeling of the reactor, there are two distributor options: bubble cap and perforated plate. The former allows the specification of the number of orifices and bubble caps, orifice discharge coefficient, and orifice diameter. The latter allows the selection of the orifice number, orifice discharge coefficient, and orifice diameter. Figure 3 depicts the comparison between the bubble cap and perforated plate distributors related to the distributor pressure drop (ΔP_d) over the total pressure drop over the bed (ΔP_t). For the first case, three bubble caps, 20 cap orifices, and a 3 mm cap orifice diameter were chosen, and the

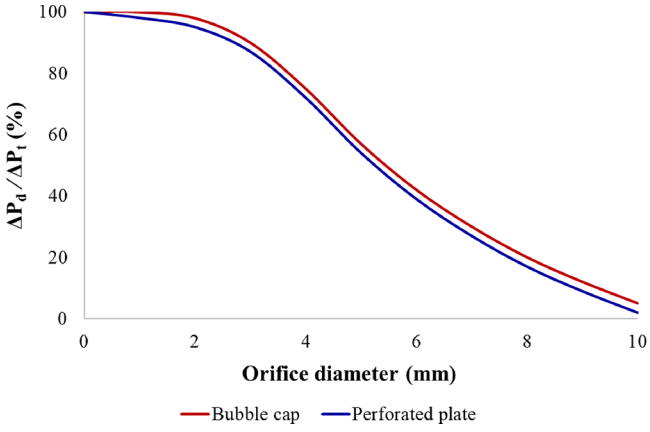

Figure 3. Effect of FBR distributor parameters on the effects of pressure drop.

https://doi.org/10.1021/acs.iecr.2c04379
Ind. Eng. Chem. Res. 2023, 62, 6386−6393

performance parameters were compared while varying the orifice diameter. In the second case, a range of 1 to 10 mm was selected for the orifice size and a standard orifice discharge coefficient of 0.65 was implemented.[44]

The results show that the $\Delta P_d/\Delta P_t$ percentage for the FBR is similar for both cases of bubble cap-perforated plate distributor, regardless of possessing constant number of orifices and orifice size. The perforated plate has a slightly lower percentage compared to the bubble cap. Yang[45] found that the perforated plate configuration is easier to construct and scale up; however, it can suffer from weeping of the bed into plenum, which is thermal distortion. On the other hand, the advantages of the bubble cap configuration are the capacity to apply the cap as a stiffening ring and a desirable turndown ratio. Nevertheless, it can be difficult to prevent the stagnant regions. Therefore, the bubble cap distributor plate would be the optimum selection based on the above.

Figure 4 shows how the behavior of the FBR model varies with changing the bed diameter, against the solid volume

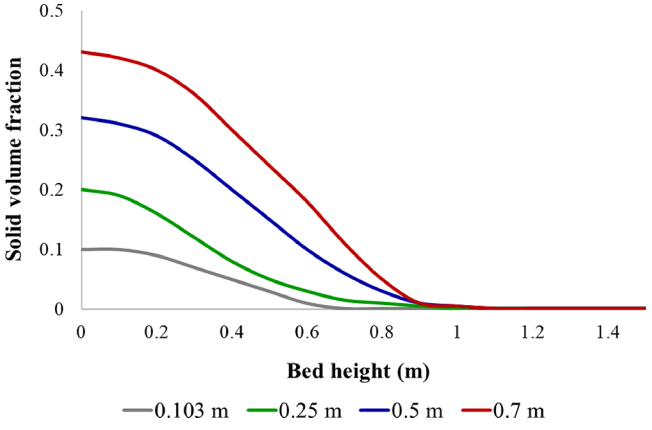

Figure 4. Effect of FBR diameter on the solid volume fraction with bed height.

fraction. All other parameters were maintained continuous while varying the bed diameter from 0.103 to 1.5 m. The results show that as the diameter of the FBR increases, the total mass of particles in the system also increases while the pressure drop is constant. Furthermore, the mean solid volume fraction in the FBR diminishes with the bed diameter and height for a constant fuel rate. The solid volume faction will continuously stay constant in the dense bed zone prior to significantly declining in the freeboard region for a specific superficial velocity.[46]

Sarker et al.[47] found that as the bed diameter decreases, the minimum fluidization velocity also decreases. However, varying the bed height had negligible effects on the minimum fluidization velocity. Furthermore, by keeping the solid holdup and gas feed rate constant, it was observed that the solid volume fraction in the dense bed rises as the bed diameter increases. This is due to the transition of the regime from bubbling to pneumatic transport. From the results obtained, the ratio of bed height to diameter is imperative to determine the size of the fluidized bed. A compromise should be made between the kinetics and hydrodynamics to permit a sufficient residence time for reactions to be completed. This is an influential design consideration in FBR reactors using process simulation modeling.

The effect of catalyst loading in the FBR can have a significant effect on the pyrolytic yield of oil. Figure 5 displays

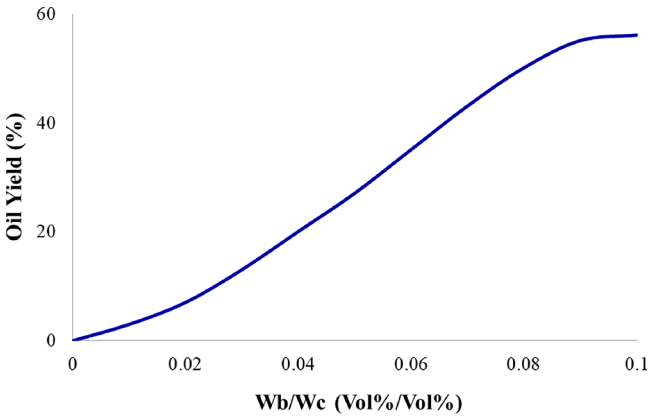

Figure 5. Effect of catalyst loading on the pyrolytic oil yield.

the effects of the ratio of bed weight (W_b) to catalyst weight (W_c) on the liquid oil yield obtained in the FBR during the pyrolysis reaction. During the study, the temperature in the reaction bed was maintained at 700 °C with all other bed and reaction parameters kept constant. From the results, it can be observed that there are negligible amounts of oil produced at lower catalyst amounts. Furthermore, as the weight of catalyst is increased, the pyrolytic oil yield further increased and subsequently stabilized at W_b/W_c ratios of approximately 0.09 and greater. Similar results were obtained by Zhang et al.,[48] which showed that almost no aromatic HCs were observed in the oil yield without the catalyst. Moreover, the use of the catalyst gives rise to a remarkable increase in aromatic HC yield compared with no catalyst, and it was observed that the carbon and hydrogen yields of individual and total aromatic HCs increase dramatically over the ranges of catalyst loading studied. This can be explained by the fact that more catalyst loading amount can provide more active sites for the cracking and deoxygenation while increasing the relative residence time of primary pyrolytic vapors passing through it.

CONCLUSIONS

LLDPE signifies a large quantity of PSW, as well as other PO plastics. The pyrolysis of plastics can accomplish environmentally friendly conversion of PSW into highly valuable fuels and chemicals. In this work, the pyrolysis of LLDPE in an FBR was investigated using process simulation modeling. The comprehensive model operated at 600 and 700 °C to investigate the pyrolytic oil and wax yield. The results showed that the oil yield decreased from 600 to 700 °C. This is because of an increase in the PO polymer matrix's vibration leading to an increase in temperature and absorbed thermal energy. Furthermore, at 700 °C, negligible wax formation and greater yields of gaseous products were observed, which is beneficial in controlling the accumulated PW, via thermochemical conversion technologies, because of the vast proportion of polyethylene present in the stream. The detailed process simulation model was compared with experimental data under the same technology and conditions, and it was found that a less than 10% discrepancy was observed between the two sets of data, suggesting a good validation between the two studies. In addition, the pyrolysis oil studied showed the diesel fuel lumped HC range (C_{10}–C_{19}) to be between

https://doi.org/10.1021/acs.iecr.2c04379
Ind. Eng. Chem. Res. 2023, 62, 6386−6393

approximately 40 and 63%. Hence, the pyrolytic oil obtained at 700 °C can be processed further to be regarded as an appropriate substitute for diesel fuel following compliance with the standards for market value. Further results pertaining to the distributor parameters showed that a bubble cap distributor plate would be the optimum choice due to a better turndown ratio and that as the diameter of the FBR increases, the total mass of particles in the system also increases. The current simulation has proven that it can successfully predict the pyrolysis of LLDPE in an FBR. Future work can be directed toward implementing the simulation for other thermochemical methodologies and with different feedstocks and catalysts, in order to enhance the understanding of the different processes.

AUTHOR INFORMATION

Corresponding Authors

Achilleas Constantinou − *Department of Chemical Engineering, Cyprus University of Technology, 3036 Limassol, Cyprus;* orcid.org/0000-0002-7763-9481; Email: a.konstantinou@cut.ac.uk

Sultan M. Al-Salem − *Environment & Life Sciences Research Centre, Kuwait Institute for Scientific Research (KISR), Safat 13109, Kuwait;* orcid.org/0000-0003-0652-4502; Email: ssalem@kisr.edu.kw

Authors

Sanaa Hafeez − *School of Engineering and Materials Science, Queen Mary University of London, London E1 4NS, United Kingdom*

Maarten Van Haute − *Q8 Research, KRPT B.V., 3198 Rotterdam, Netherlands*

Complete contact information is available at: https://pubs.acs.org/10.1021/acs.iecr.2c04379

Author Contributions

S.H.: data analysis, initial and final draft preparation; S.M.A-S.: conceptualization, data analysis, initial and final draft preparation; M.V.H.: final draft review; A.C.: data analysis, initial and final draft preparation.

Notes

The authors declare no competing financial interest.

ACKNOWLEDGMENTS

The lead author/project leader would like to thank the Kuwait Foundation for the Advancement of Sciences (KFAS) and the Kuwait Institute for Scientific Research (KISR) for funding and supporting this research project through the Grant for Project EM114C (AP21-45EC-01). The Project Leader would also like to dedicate this report to Mr. Majed Al-Wadi who has retired from service as a Principal Senior Research Technician after a fruitful and prosperous 33-year career at KISR, ending his work with duties assigned to this project.

REFERENCES

(1) Esso, S. B. E.; Xiong, Z.; Chaiwat, W.; Kamara, M. F.; Longfei, X.; Xu, J.; Ebako, J.; Jiang, L.; Su, S.; Hu, S. Review on synergistic effects during co-pyrolysis of biomass and plastic waste: Significance of operating conditions and interaction mechanism. *Biomass Bioenergy* **2022**, *159*, No. 106415.

(2) PlasticsEurope, E., *Plastics—The Facts 2019. An Analysis of European Plastics Production, Demand and Waste Data*; PlasticEurope https://www. plasticseurope. org/en/resources/publications/1804-plastics-facts-2019 2019.

(3) Jambeck, J. R.; Geyer, R.; Wilcox, C.; Siegler, T. R.; Perryman, M.; Andrady, A.; Narayan, R.; Law, K. L. Plastic waste inputs from land into the ocean. *Science* **2015**, *347*, 768−771.

(4) Sharuddin, S. D. A.; Abnisa, F.; Daud, W. M. A. W.; Aroua, M. K. A review on pyrolysis of plastic wastes. *Energy Convers. Manage.* **2016**, *115*, 308−326.

(5) Jiang, J.; Shi, K.; Zhang, X.; Yu, K.; Zhang, H.; He, J.; Ju, Y.; Liu, J. From plastic waste to wealth using chemical recycling: A review. *J. Environ. Chem. Eng.* **2022**, *10*, No. 106867.

(6) Antelava, A.; Jablonska, N.; Constantinou, A.; Manos, G.; Salaudeen, S. A.; Dutta, A.; Al-Salem, S. M. Energy potential of plastic waste valorization: A short comparative assessment of pyrolysis versus gasification. *Energy Fuels* **2021**, *35*, 3558−3571.

(7) Fürsatz, K.; Fuchs, J.; Benedikt, F.; Kuba, M.; Hofbauer, H. Effect of biomass fuel ash and bed material on the product gas composition in DFB steam gasification. *Energy* **2021**, *219*, No. 119650.

(8) Hafeez, S.; Aristodemou, E.; Manos, G.; Al-Salem, S. M.; Constantinou, A. Modelling of packed bed and coated wall microreactors for methanol steam reforming for hydrogen production. *RSC Advances* **2020**, *10* (68), 41680−92.

(9) Kan, T.; Strezov, V.; Evans, T.; He, J.; Kumar, R.; Lu, Q. Catalytic pyrolysis of lignocellulosic biomass: A review of variations in process factors and system structure. *Renewable Sustainable Energy Rev.* **2020**, *134*, No. 110305.

(10) Kunwar, B.; Cheng, H.; Chandrashekaran, S. R.; Sharma, B. K. Plastics to fuel: a review. *Renewable Sustainable Energy Rev.* **2016**, *54*, 421−428.

(11) Al-Salem, S.; Antelava, A.; Constantinou, A.; Manos, G.; Dutta, A. A review on thermal and catalytic pyrolysis of plastic solid waste (PSW). *J. Environ. Manage.* **2017**, *197*, 177−198.

(12) Antelava, A.; Damilos, S.; Hafeez, S.; Manos, G.; Al-Salem, S. M.; Sharma, B. K.; Kohli, K.; Constantinou, A. Plastic solid waste (PSW) in the context of life cycle assessment (LCA) and sustainable management. *Environ. Manage.* **2019**, *64*, 230−244.

(13) Buekens, A. Introduction to feedstock recycling of plastics. *Feedstock Recycl. Pyrolysis Waste Plast.* **2006**, *6*, 1−41.

(14) Xayachak, T.; Haque, N.; Parthasarathy, R.; King, S.; Emami, N.; Lau, D.; Pramanik, B. K. Pyrolysis for Plastic Waste Management: An Engineering Perspective. *J. Environ. Chem. Eng.* **2022**, No. 108865.

(15) Hafeez, S.; Pallari, E.; Manos, G.; Constantinou, A., Catalytic conversion and chemical recovery. In *Plastics to energy*, Elsevier: 2019; pp. 147−172.

(16) Hasan, M.; Rasul, M.; Jahirul, M.; Khan, M. Fast pyrolysis of macadamia nutshell in an auger reactor: Process optimization using response surface methodology (RSM) and oil characterization. *Fuel* **2023**, *333*, No. 126490.

(17) Jahirul, M.; Rasul, M.; Schaller, D.; Khan, M.; Hasan, M.; Hazrat, M. Transport fuel from waste plastics pyrolysis−A review on technologies, challenges and opportunities. *Energy Convers. Manage.* **2022**, *258*, No. 115451.

(18) Kaminsky, W.; Kim, J.-S. Pyrolysis of mixed plastics into aromatics. *J. Anal. Appl. Pyrolysis* **1999**, *51*, 127−134.

(19) Antelava, A.; Pallari, E.; Manos, G.; Constantinou, A., Design and limitations in polymer cracking fluidized beds for energy recovery. In *Plastics to Energy*, Elsevier: 2019; pp. 221−231, DOI: 10.1016/B978-0-12-813140-4.00008-X.

(20) Al-Rumaihi, A.; Shahbaz, M.; Mckay, G.; Mackey, H.; Al-Ansari, T. A review of pyrolysis technologies and feedstock: A blending approach for plastic and biomass towards optimum biochar yield. *Renewable Sustainable Energy Rev.* **2022**, *167*, No. 112715.

(21) Qianshi, S.; Wei, Z.; Xiaowei, W.; Xiaohan, W.; Haowen, L.; Zixin, Y.; Yue, Y.; Guangqian, L. Comprehensive effects of different inorganic elements on initial biomass char-CO2 gasification reactivity in micro fluidised bed reactor: Theoretical modeling and experiment analysis. *Energy* **2023**, *262*, No. 125379.

(22) Salaudeen, S. A.; Al-Salem, S. M.; Sharma, S.; Dutta, A. Pyrolysis of High-Density Polyethylene in a Fluidized Bed Reactor:

Pyro-Wax and Gas Analysis. *Ind. Eng. Chem. Res.* **2021**, *60*, 18283−18292.
(23) Al-Salem, S.; Van Haute, M.; Karam, H.; Hakeem, A.; Meuldermans, W.; Patel, J.; Hafeez, S.; Manos, G.; Constantinou, A. Fuel Range Properties of Oil and Wax Obtained from Catalytic Pyrolysis of Linear Low-Density Polyethylene in a Fluidized Bed Reactor (FBR). *Ind. Eng. Chem. Res.* **2022**, *61*, 16383−16392.
(24) Abomohra, A. E.-F.; Sheikh, H. M.; El-Naggar, A. H.; Wang, Q. Microwave vacuum co-pyrolysis of waste plastic and seaweeds for enhanced crude bio-oil recovery: Experimental and feasibility study towards industrialization. *Renewable Sustainable Energy Rev.* **2021**, *149*, No. 111335.
(25) Ismail, H. Y.; Abbas, A.; Azizi, F.; Zeaiter, J. Pyrolysis of waste tires: A modeling and parameter estimation study using Aspen Plus®. *Waste Manage.* **2017**, *60*, 482−493.
(26) Singh, M.; Salaudeen, S. A.; Gilroyed, B. H.; Dutta, A. Simulation of biomass-plastic co-gasification in a fluidized bed reactor using Aspen plus. *Fuel* **2022**, *319*, No. 123708.
(27) Ryu, H. W.; Tsang, Y. F.; Lee, H. W.; Jae, J.; Jung, S.-C.; Lam, S. S.; Park, E. D.; Park, Y.-K. Catalytic co-pyrolysis of cellulose and linear low-density polyethylene over MgO-impregnated catalysts with different acid-base properties. *Chem. Eng. J.* **2019**, *373*, 375−381.
(28) Ding, K.; Zhong, Z.; Wang, J.; Zhang, B.; Fan, L.; Liu, S.; Wang, Y.; Liu, Y.; Zhong, D.; Chen, P.; Ruan, R. Improving hydrocarbon yield from catalytic fast co-pyrolysis of hemicellulose and plastic in the dual-catalyst bed of CaO and HZSM-5. *Bioresour. Technol.* **2018**, *261*, 86−92.
(29) Lai, J.; Meng, Y.; Yan, Y.; Lester, E.; Wu, T.; Pang, C. H. Catalytic pyrolysis of linear low-density polyethylene using recycled coal ash: Kinetic study and environmental evaluation. *Korean J. Chem. Eng.* **2021**, *38*, 2235−2246.
(30) Arena, U.; Di Gregorio, F. Energy generation by air gasification of two industrial plastic wastes in a pilot scale fluidized bed reactor. *Energy* **2014**, *68*, 735−743.
(31) Li, S.; Sanna, A.; Andresen, J. M. Influence of temperature on pyrolysis of recycled organic matter from municipal solid waste using an activated olivine fluidized bed. *Fuel Process. Technol.* **2011**, *92*, 1776−1782.
(32) Sun, J.; Wang, W.; Liu, Z.; Ma, Q.; Zhao, C.; Ma, C. Kinetic study of the pyrolysis of waste printed circuit boards subject to conventional and microwave heating. *Energies* **2012**, *5*, 3295−3306.
(33) Xu, F.; Wang, B.; Yang, D.; Hao, J.; Qiao, Y.; Tian, Y. Thermal degradation of typical plastics under high heating rate conditions by TG-FTIR: Pyrolysis behaviors and kinetic analysis. *Energy Convers. Manage.* **2018**, *171*, 1106−1115.
(34) Rana, S.; Parikh, J. K.; Mohanty, P. Thermal degradation and kinetic study for different waste/rejected plastic materials. *Korean J. Chem. Eng.* **2013**, *30*, 626−633.
(35) Yan, Y.; Meng, Y.; Tang, L.; Kostas, E. T.; Lester, E.; Wu, T.; Pang, C. H. Ignition and kinetic studies: the influence of lignin on biomass combustion. *Energy Fuels* **2019**, *33*, 6463−6472.
(36) Dubdub, I.; Al-Yaari, M. Pyrolysis of low density polyethylene: kinetic study using TGA data and ANN prediction. *Polymer* **2020**, *12*, 891.
(37) Conesa, J. A.; Font, R. Kinetic severity function as a test for kinetic analysis. Application to polyethylene pyrolysis. *Energy Fuels* **1999**, *13*, 678−685.
(38) Tasirin, S.; Geldart, D. Entrainment of FCC from fluidized beds—a new correlation for the elutriation rate constants Ki∞. *Powder Technol.* **1998**, *95*, 240−247.
(39) Park, K.-B.; Jeong, Y.-S.; Guzelciftci, B.; Kim, J.-S. Characteristics of a new type continuous two-stage pyrolysis of waste polyethylene. *Energy* **2019**, *166*, 343−351.
(40) Al-Salem, S.; Dutta, A.; Al-Wadi, M. H., System for processing waste. Google Patents: 2021.
(41) Sabogal, O. S.; Valin, S.; Thiery, S.; Salvador, S. Design and thermal characterization of an induction-heated reactor for pyrolysis of solid waste. *Chem. Eng. Res. Des.* **2021**, *173*, 206−214.
(42) Al-Salem, S.; Lettieri, P.; Baeyens, J. The valorization of plastic solid waste (PSW) by primary to quaternary routes: From re-use to energy and chemicals. *Prog. Energy Combust. Sci.* **2010**, *36*, 103−129.
(43) Al-Salem, S.; Al-Nasser, A.; Al-Dhafeeri, A. Multi-variable regression analysis for the solid waste generation in the State of Kuwait. *Process Saf. Environ. Prot.* **2018**, *119*, 172−180.
(44) Kappagantula, R. V.; Ingram, G. D.; Vuthaluru, H. B. Application of Aspen Plus fluidized bed reactor model for chemical Looping of synthesis gas. *Fuel* **2022**, *324*, No. 124698.
(45) Yang, W.-C., *Handbook of fluidization and fluid-particle systems*. CRC press: 2003, DOI: 10.1201/9780203912744.
(46) Levenspiel, O., *Chemical reaction engineering*. John wiley & sons: 1998.
(47) Sarker, R.; Rahman, M.; Love, N.; Choudhuri, A. In *Effect of bed height, bed diameter and particle shape on minimum fluidization in a gas-solid fluidized bed, 50th AIAA Aerospace Sciences Meeting including the New Horizons Forum and Aerospace Exposition*, 2012; p 644.
(48) Zhang, B.; Zhong, Z.; Zhang, J.; Ruan, R. Catalytic fast co-pyrolysis of biomass and fusel alcohol to enhance aromatic hydrocarbon production over ZSM-5 catalyst in a fluidized bed reactor. *J. Anal. Appl. Pyrolysis* **2018**, *133*, 147−153.